

# Incidental Cardiac and Pericardial Abnormalities on Chest CT

Soo-Hyun Lee, MD,\*† Joon Beom Seo, MD,\* Joon-Won Kang, MD,\* Eun Jin Chae, MD,\*  
Seong Hoon Park, MD,\* and Tae-Hwan Lim, MD\*

**Objective:** Although there has been an increasing interest in diagnosing cardiac and pericardial diseases using electrocardiogram-gated cardiac computed tomography (CT), radiologists tend to neglect or overlook many incidentally detected abnormalities on conventional, nongated chest CT. The objective of this study is to describe the imaging appearance and clinical significance of such cardiac or pericardial diseases.

**Conclusions:** Recognition and detection of various cardiac and pericardial abnormalities on chest CT as the evaluation of noncardiac disease is important for its early diagnosis and proper management.

**Key Words:** CT, thoracic, heart, pericardium

(*J Thorac Imaging* 2008;23:216–226)

Advances in computed tomography (CT) and magnetic resonance imaging have brought renewed interest to the field of cardiac imaging, and radiologists are realizing that they have created new opportunities for the early diagnosis of various diseases. In particular, CT imaging of the heart is affected as recently developed multidetector row CT provides high-quality, motion-free images of the heart. However, as routine chest CT is obtained without electrocardiogram-gating, interpretation of the images focusing on pulmonary disease still may result in ignorance or neglect of many cardiac and pericardial abnormalities. Detection of cardiac and pericardial diseases on routine chest CT is important because occult cardiac disease alters a patient's clinical course and outcome. This article reviews the cardiac and pericardial abnormalities detected incidentally on routine chest CT.

## ISCHEMIC HEART DISEASE

Ischemic heart disease is most commonly caused by atherosclerotic coronary artery obstruction. The process

of an acute myocardial infarction results in a series of changes in the left ventricular (LV) myocardium, characterized by acute ischemia, myocardial death, and chronic remodeling.<sup>1</sup> Although early studies performed on conventional, single-slice, whole-body CT scanners, demonstrated that acute myocardial infarction could be identified as a region of lower attenuation than normal enhanced myocardium, diagnostic accuracy using the conventional CT is very low in diagnosing the acute myocardial events as the cause of acute chest pain. However, incidental detection of coronary calcification identifies individuals at risk for acute coronary events.<sup>2,3</sup> Coronary artery calcification correlates highly with plaque burden but its relationship to plaque instability is low (Fig. 1). A mild degree of calcification characterizes patients with acute coronary events, whereas diffused high-attenuation calcific plaques are associated with chronic coronary events.<sup>4</sup>

LV myocardial aneurysms are relatively common sequelae of transmural myocardial infarction. Focal aneurysmal dilatation of a portion of the ventricular wall is found in 8% to 12% of patients who sustain an acute myocardial infarction. True aneurysms are defined as areas of thinned myocardium, which are dyskinetic and involve the full thickness of the wall. On the other hand, pseudoaneurysms are a result of rupture of the ventricular free wall, contained by overlying adherent pericardium.<sup>5</sup> They typically have a neck narrower than the diameter of the aneurysm and are more often located in the posterior and lateral wall segments, in contrast to true aneurysms, which are more often seen in the anterior wall and apex, and have a wide neck (Fig. 2). More importantly, pseudoaneurysms have a higher risk of rupture and thus, a surgical approach for its management is often undertaken. Whether seeming as focal or global contour abnormalities, LV aneurysms could have curvilinear myocardial calcification (Fig. 2) and subendocardial fatty replacement (Fig. 3) in area of true aneurysm<sup>6</sup> or curvilinear dark line indicating fibrosis or fatty metaplasia.<sup>7</sup> Myocardial calcification is a reliable sign of previous myocardial infarction. Septal involvement and regional myocardial thinning help to differentiate these lesions from those of calcific pericarditis.<sup>8</sup>

Occasionally, mural thrombus is seen as filling defect within the ventricular cavity subjacent to areas of myocardial thinning or dyskinesia.<sup>9</sup> Thrombus may have the same appearance (intracavitary filling defects) as

From the \*Department of Radiology and Research Institute of Radiology, University of Ulsan College of Medicine, Asan Medical Center, Seoul; and †Department of Radiology, National Cancer Center, Gyeonggi-do, Korea.

Reprints: Joon Beom Seo, MD, Department of Radiology and Research Institute of Radiology, University of Ulsan College of Medicine, Asan Medical Center, 388-1 Pungnap-2-dong, Songpa-gu, Seoul, Republic of Korea (e-mail: seojb@amc.seoul.kr).

Copyright © 2008 by Lippincott Williams & Wilkins

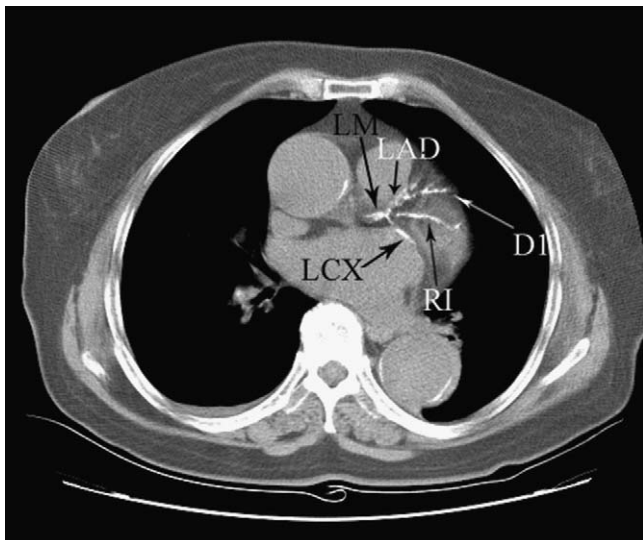


**FIGURE 1.** Coronary artery calcification in a 78-year-old woman with abdominal aortic aneurysm. Extensive calcifications are noted in the left coronary artery tree (arrows). Atherosclerotic calcification is also seen along the aortic wall. (LM, left main coronary artery; LAD, left anterior descending artery; LCx, left circumflex artery; RI, ramus intermedius; D1, first diagonal branch).

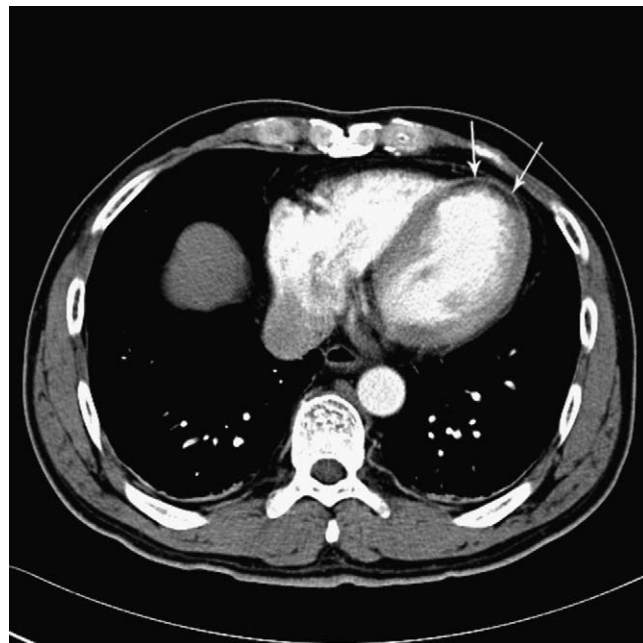


**FIGURE 3.** LV aneurysm in a 60-year-old man. A dark line (arrows), indicating fibro-fatty change, is noted along the thin apical myocardium.

papillary muscle. However, papillary muscles enhance with contrast administration; thrombi do not.

### VALVULAR HEART DISEASE

Although the incidence of valvular heart disease has been significantly decreased since the antibiotic therapy was introduced, chronic mitral and aortic valve disease

continues to be found in the adult population. There are limitations to the demonstration of morphologic abnormalities of each cardiac valve on chest CT because of the complex orientation of the cardiac valves and the limited temporal CT resolution. However, an understanding of the hemodynamic adaptation of the myocardium and the cardiac chambers may cause suspicion of valvular heart disease. This myocardial adaptation causes dilatation or hypertrophy of each chamber, which is normally almost equal size. Although it is unusual for CT to be used as a first line of diagnosis in these patients, it does provide important morphologic and physiologic information concerning chamber size, myocardial mass, and pulmonary blood flow and pressure. Furthermore, its exquisite sensitivity to the presence of calcium is very helpful for identifying and characterizing chronic valvular disease.<sup>10</sup>

### Mitral Valve Diseases

Chronic rheumatic carditis is the most common etiology of mitral stenosis/regurgitation. The slowly progressive process of reactive fibrosis results in mitral stenosis. The mitral leaflets then thicken, calcify, and fuse (Fig. 4). Chronic mitral stenosis results in left atrial and left atrial appendage dilatation in contrast with a normal LV. Calcification of the left atrium is a relatively common finding in patients with long-lasting rheumatic valve disease (Fig 5).<sup>11</sup> The chronic left atrial hypertension results in pulmonary vein dilatation, and eventually in pulmonary hypertension (Fig. 4). In patients with pulmonary hypertension, the right ventricular (RV) myocardium hypertrophies, resulting in thickening of the RV free wall and septal myocardium. In cases with

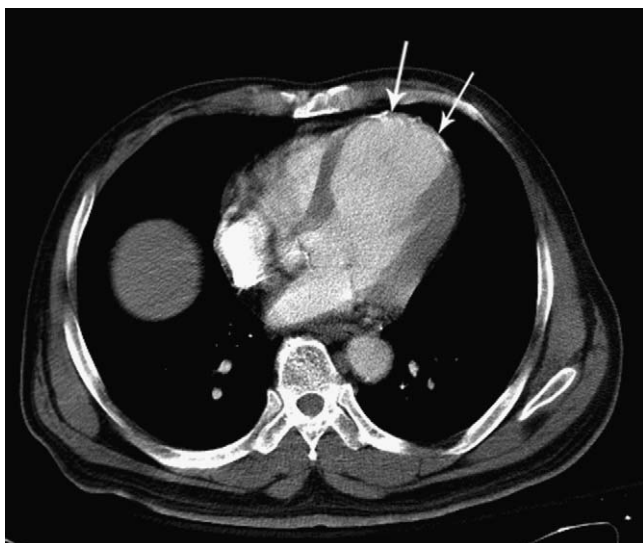


**FIGURE 2.** LV aneurysm in a 62-year-old man with abdominal aortic aneurysm. The paper-thin apical myocardium is dilated, and dystrophic curvilinear calcifications (arrows) are lined on the thinned LV wall.

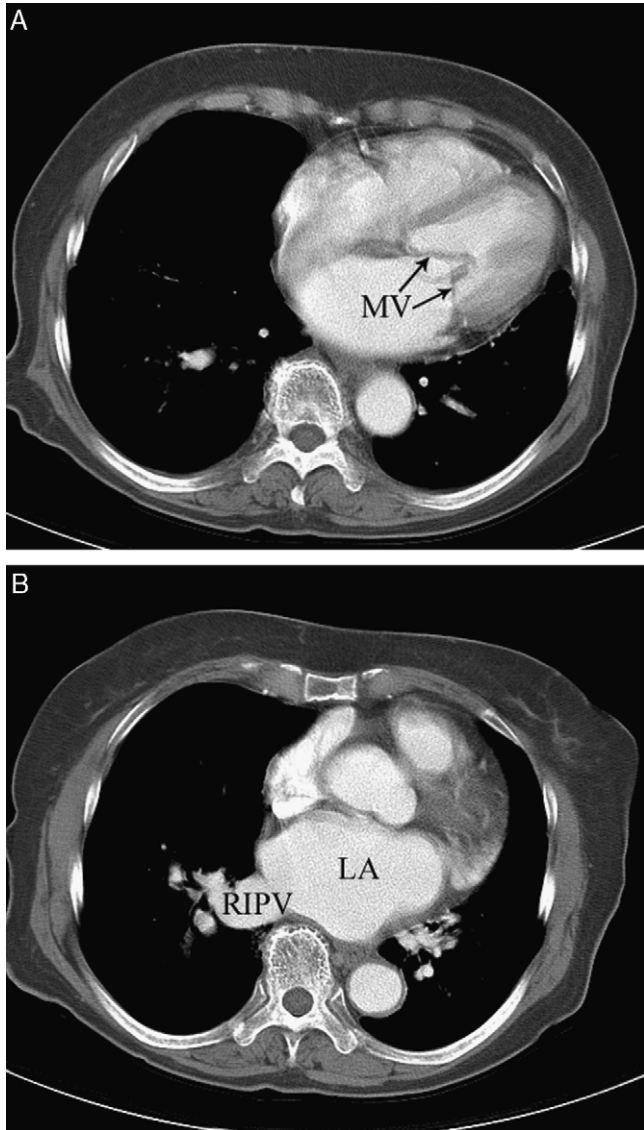


**FIGURE 4.** Mitral stenosis in a 79-year-old woman who underwent chest CT because of an abnormal chest radiograph. A, Her mitral valve (MV) leaflets (arrows) are thickened. B, The left atrium (LA) is dilated and hypertrophied. The right inferior pulmonary vein (RIPV) is dilated.

right atrial hypertension, flattening and posterior bowing of the interatrial septum may also be seen. RV failure in these patients is manifested by coronary sinus, inferior vena cava, and hepatic vein and azygos vein dilatation.

Mitral annulus calcification is a chronic, non-inflammatory, degenerative process of the fibrous support structure of the mitral valve. Mitral annulus calcification may not alter the function of mitral valve, but it is important as an additional marker of atherosclerosis (Fig 6).<sup>10</sup> Extensive degenerative calcification of the mitral valvular annulus may extend to the valve leaflets, resulting in a variety of valvular diseases, including mitral valve stenosis.<sup>12</sup> In clinical practice, it is not difficult to differentiate mitral annulus calcifications from mitral

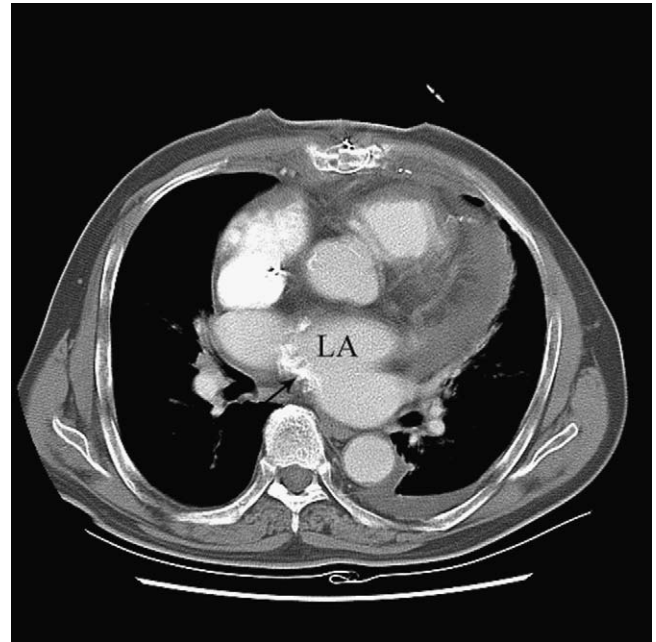


**FIGURE 5.** Left atrial wall calcification in a 73-year-old man with a history of mitral valve replacement surgery. Calcifications (arrow) are seen along the posterior wall of the left atrium (LA) on postoperative CT.

valvular calcification. Mitral annulus calcification is noted along the atrioventricular groove that is the outer ring of mitral valve, whereas mitral valvular calcification

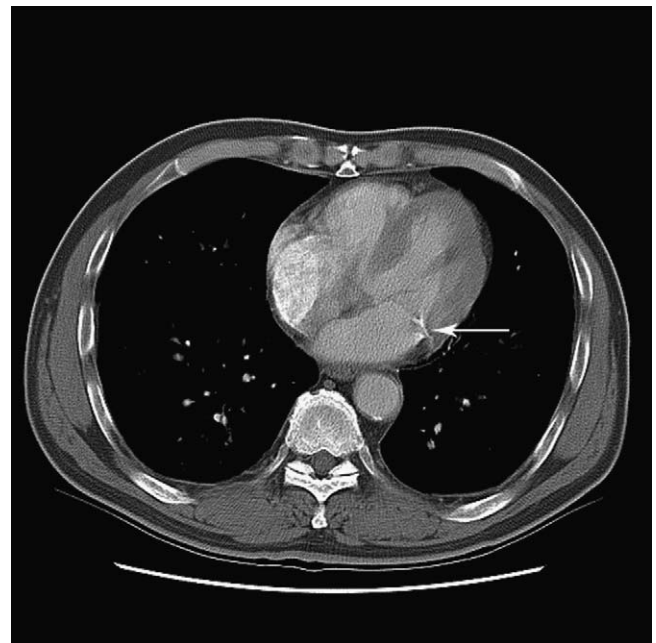


**FIGURE 6.** Mitral annulus calcification in a 65-year-old man who underwent CT for the metastasis work-up of colon cancer. Focal calcifications are noted in the mitral annulus (arrow) and descending thoracic aorta. The mitral calcification is important as an additional marker of atherosclerosis.

is actually located on mitral leaflets. Differentiation of the lesion from the calcification of left circumflex artery is also easy because it is usually thicker and located deeper than coronary artery calcification.

Chronic mitral regurgitation results in adaptation of the left atrium and ventricle to the volume load. Thus left atrial and ventricular dilatation is the rule. LV mass increases with the increased chamber volume, resulting in thickening of the LV myocardium. When the mitral leaflets are fixed and fibrosis extends to the chordae tendinae, which becomes thickened and fused, mitral regurgitation may coexist with mitral stenosis. In acute mitral regurgitation, especially complicated with acute myocardial infarction, cardiac chamber size is not altered; the heart may seem normal. However, the predominant findings are the changes of severe left atrial hypertension and interstitial pulmonary edema.

### Aortic Valve Diseases

Aortic stenosis can occur at, below or above the aortic valve. The causes of aortic stenosis are congenital, degenerative, and rheumatic (Fig. 7). Subvalvular and supra-ventricular aortic stenoses are usually congenital in origin.<sup>13</sup> The CT diagnosis of aortic stenosis is based on the demonstration of LV hypertrophy, mild-to-moderate dilatation of the ascending aorta, and calcification of the aortic valve.<sup>14,15</sup>

In patients with congenital aortic valve disease, early shear stress owing to turbulent flows causes an early fibrocalcific process, which results in a thickening and early calcification of the valve leaflets. CT allows differentiation between annular and leaflet calcification. In the former circumstance, aortic sclerosis may be present, but a transvalvular gradient is commonly not found. On the other hand, there is a strong association between aortic leaflet calcification and a gradient across the valve.

Aortic regurgitation is diagnosed on CT by recognition of LV and aortic dilatation. Thus, milder forms of the disease may be overlooked, and grading of the severity of the valvular dysfunction is inaccurate. In aortic regurgitation, CT may be helpful by demonstrating the severity and extent of aortic dilatation.

### Pulmonary Valve Disease

In patients with pulmonary stenosis, the main pulmonary artery is dilated owing to the jet effect of blood traversing the narrowed valve orifice and to turbulent blood flow in the postvalvular portion of the pulmonary artery. Asymmetric prominence of the left pulmonary artery is a frequent finding of pulmonary stenosis (Fig. 8) also found in patients with patent ductus arteriosus (PDA) and in patients with hypoplasia or the absence of a right pulmonary artery.<sup>16</sup> In pulmonary stenosis, the peripheral pulmonary arteries are usually normal in caliber, but the pulmonary vascularity is increased by left to right shunt flow in PDA.

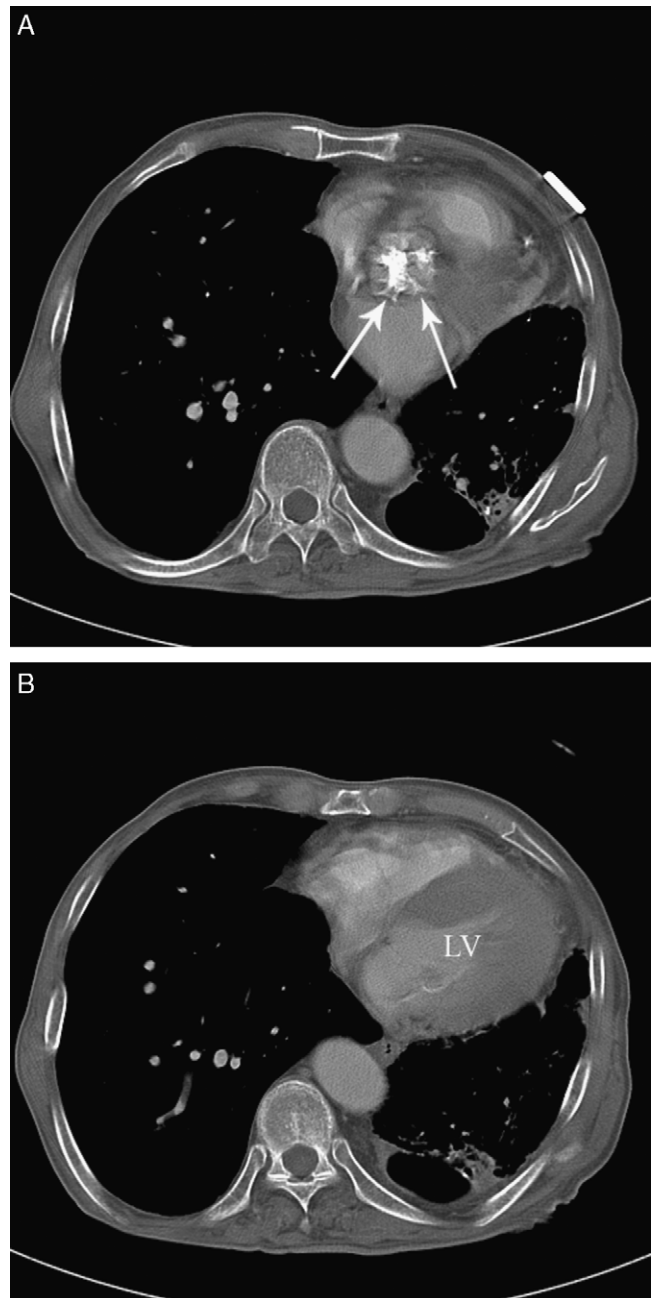


**FIGURE 7.** Aortic stenosis in a 72-year-old man who underwent CT for the evaluation of advanced pulmonary tuberculosis. A, Dense clustered calcifications (arrows) are noted on aortic valve area. B, LV is hypertrophied owing to increased afterload.

### CONGENITAL HEART DISEASES

The patients with small isolated cardiovascular defect such as atrial septal defect (ASD), ventral septal defect, PDA may have been missed and may not be discovered until adulthood. Additionally, advances in medicine have increased the life expectancy of patients with congenital heart disease, and the population of adults with congenital heart has been increased. Thus we

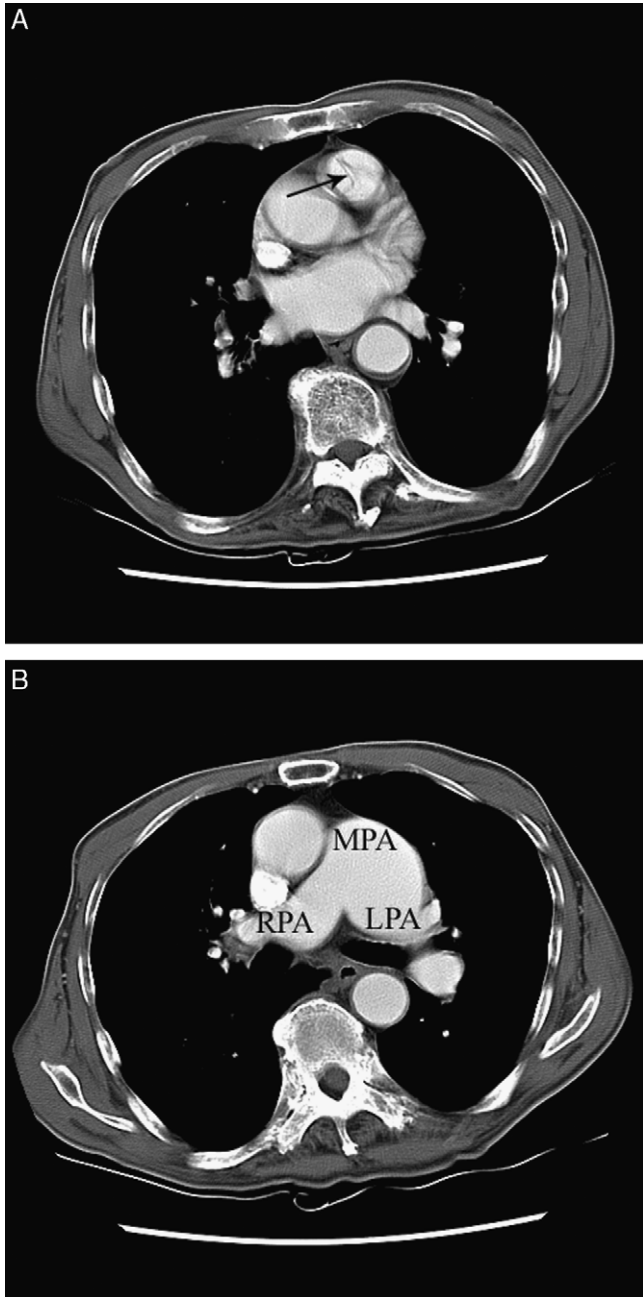


**FIGURE 8.** Pulmonary valvular stenosis in a 67-year-old man who underwent CT scanning because of an abnormal chest radiograph. A, The pulmonary valve is thickened (arrow). B, The main pulmonary artery (MPA) is enlarged owing to poststenotic dilation. The left pulmonary artery (LPA) is larger than the right (RPA).

could have more opportunity to encounter CT images of patient with congenital heart disease. Because the congenital heart disease alters the clinical manifestation or prognosis of many pulmonary diseases, the detection of congenital heart disease is helpful in the evaluation of unexplained thoracic symptoms.

ASD accounts for about one-third of cases of congenital heart disease detected in adults.<sup>17</sup> Ostium secundum ASDs are the most common type of interatrial communication located within the oval fossa. The diagnosis of ASD should be carefully made because the interatrial septum may be too thin to be delineated on CT in the region of the fossa ovalis (Fig. 9).

The ductus arteriosus in the fetus connects the proximal left pulmonary artery with the proximal part of the descending aorta just distal to the left subclavian artery. If the ductus arteriosus does not close spontaneously after birth, there is continuous flow from the descending aorta to the pulmonary arteries (Fig. 10).<sup>17</sup>

In some cases, isolated small ASD or PDA is initially detected on routine chest CT for the evaluation of pulmonary hypertension or unexplained dyspnea, or for further evaluation of bilateral hilar enlargement on chest radiograph in adulthood.<sup>18</sup>

A coronary arteriovenous fistula (CAVF) is a clinically significant congenital coronary anomaly. CAVF may be congenital or acquired. Acquired fistulae may be infectious, traumatic or iatrogenic in etiology. About 50% of CAVFs arise from the right coronary arterial tree, 42% from the left, 5% from both, and others is not specified on coronary angiography. The fistulae drain into the venous circulation in most of these patients with only small numbers of fistulae draining into the left heart. Most patients with CAVF remain asymptomatic in the first 2 decades of life, but thereafter the number of



**FIGURE 9.** ASD in a 43-year-old man. Large ASD (arrows) was noted on CT while searching the cause of the patient's dyspnea. The right atrium and ventricle are enlarged owing to the left-to-right shunt. The pulmonary artery is dilated (not shown) owing to the development of pulmonary arterial hypertension.

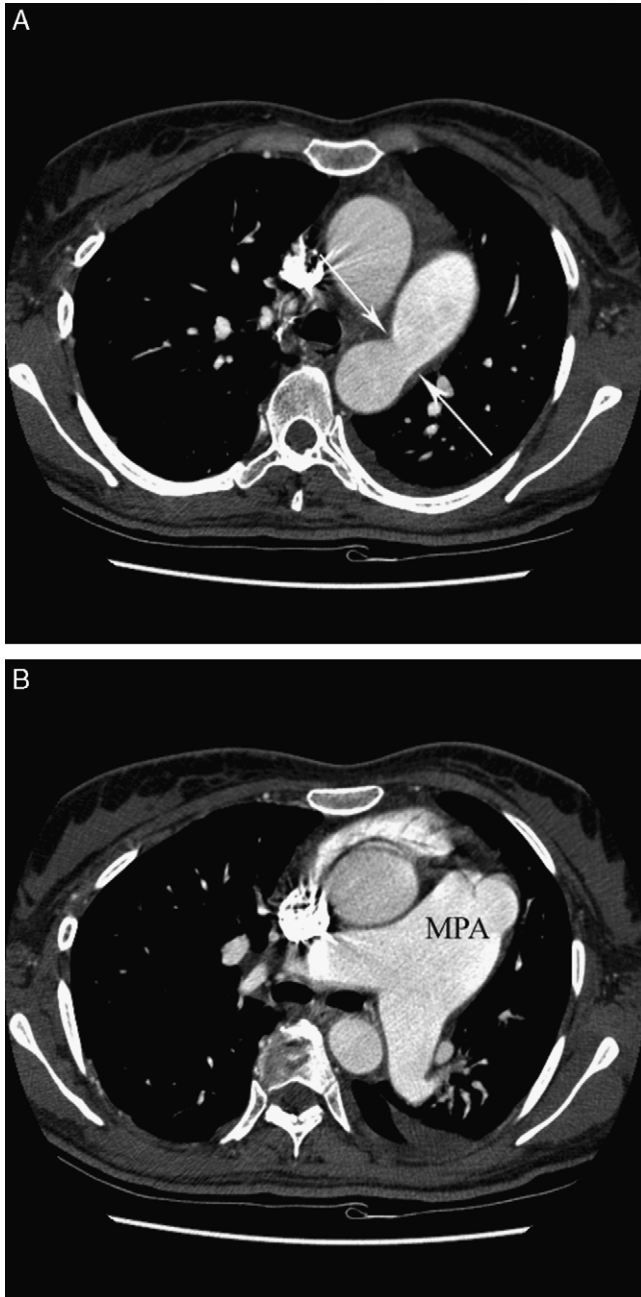


**FIGURE 10.** PDA in a 37-year-old man with dyspnea. A, A large PDA (arrow) is noted. B, The main pulmonary artery (MPA) is dilated, suggesting severe pulmonary arterial hypertension.

symptomatic individuals increases.<sup>19</sup> On CT, nodular and dilated contrast-filled structures around cardiac chambers or the pulmonary trunk, suggest CAVF (Fig. 11).

### Myocardial Abnormalities

#### Thick Myocardium

Hypertrophic cardiomyopathy is defined as idiopathic hypertrophy of the left ventricle without a primary

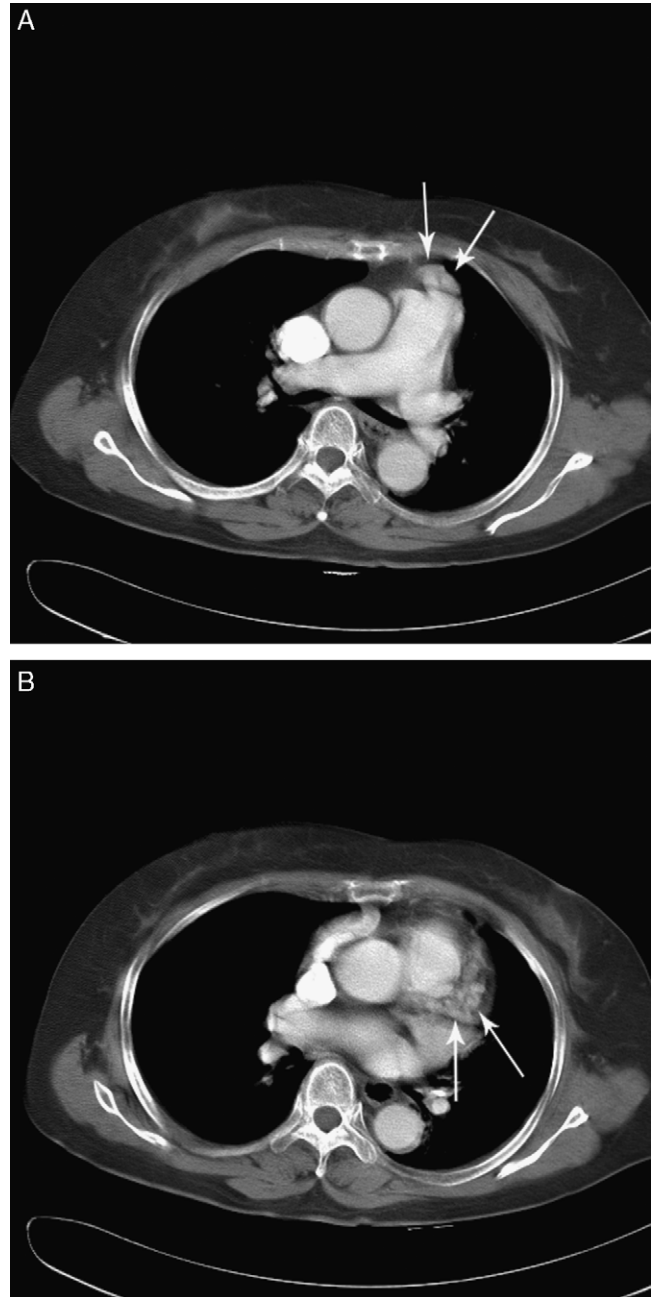


**FIGURE 11.** Coronary arteriovenous fistula in a 57-year-old woman. A, Dilated tortuous vessels (arrows) are noted anterior to main pulmonary artery. B, Serpentine vessels (arrows) are noted between right ventricular outflow tract and left atrial appendage. These abnormal vessels are confirmed as fistula from the left coronary arteries to the main pulmonary artery with coronary angiogram (not shown).

cause of LV outflow tract obstruction. The interventricular septum is the most commonly affected in the obstructive form (Fig. 12). In the concentric form, all of the myocardium is involved. Isolated noncompaction of the ventricular myocardium is characterized by an excessively prominent trabecular meshwork and deep

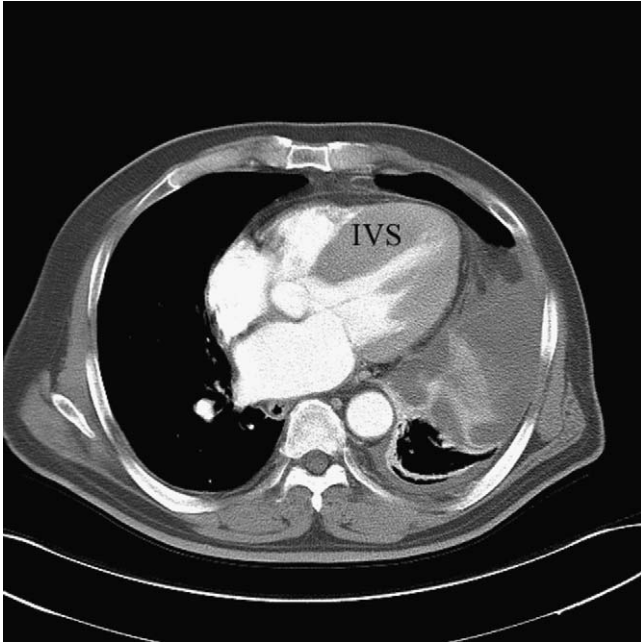


**FIGURE 12.** Hypertrophic cardiomyopathy in a 67-year-old man with renal cell carcinoma. The interventricular septum (IVS) is hypertrophied, which causes subaortic stenosis. The left pleural effusion is associated with renal cell carcinoma.

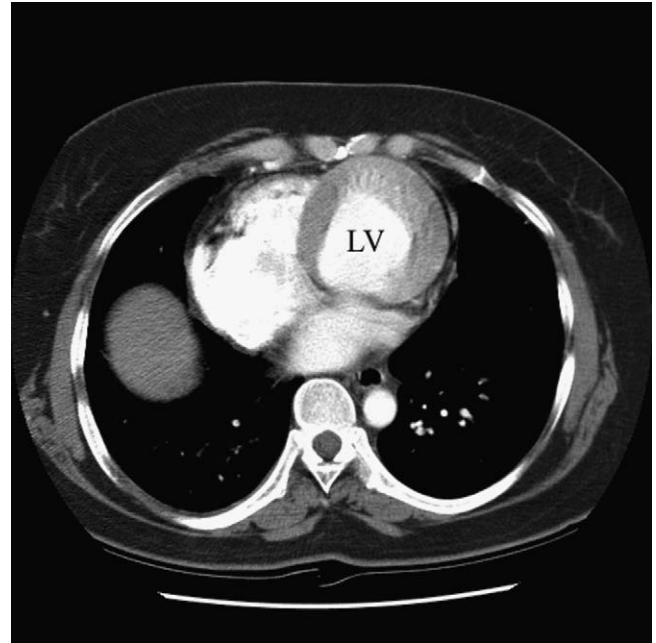


**FIGURE 13.** Myocardial noncompaction in a 43-year-old woman who underwent CT for the evaluation of the pseudocoarctation of aortic arch. LV is thickened, and its inner zone has meshlike texture as a result of noncompaction.

intertrabecular recesses (Fig. 13). This disease usually has a longer clinical course accompanied by gradually depressed LV function.<sup>20</sup> The cause of the decreased LV function is not clear, but may be related to poor ventricular perfusion caused by the presence of the trabeculations or decreased diastolic function caused by abnormal LV compliance. Other complications of myocardial noncompaction are ventricular arrhythmia and the development of mural thrombi. The thickness of normal LV myocardium on routine CT is variable because it is scanned at various phases in cardiac cycle without electrocardiogram gating. In addition, because the images are mostly reconstructed in transaxial plane, the LV myocardium is shown in oblique angle. Accordingly, it is not easy to tell mild myocardial thickening from normal myocardium scanned in systolic phase. In our clinical experience, we evaluate the whole LV myocardium carefully, because usually the CT images are scanned in various cardiac phases. We determine that the myocardium is thinned when the interventricular septal or posterior myocardium on axial image of midventricular level is thinner than 10 mm and that the myocardium is thick when it is thicker than 20 to 25 mm.

### Dense Myocardium

The interventricular septum is distinctly visible on CT in patients with severe anemia. This finding is noted in patients with glycogen and iron storage diseases and also in patients with iron overload caused by multiple blood transfusions in the presence of normal hemoglobin levels (Fig. 14).<sup>21</sup> It has been suggested that blood of normal

hemoglobin concentration and cardiac muscle have similar attenuation coefficients. Most patients with normal hemoglobin levels did demonstrate attenuation



**FIGURE 14.** Dense myocardium in a 58-year-old man with anemia. The myocardium shows higher attenuation than the ventricular chamber on unenhanced CT. The hemoglobin of this patient was 8.3 g/dL, and the hematocrit was 25.5%.

coefficients of blood and cardiac muscle that were similar. However, the blood of patients with abnormal hemoglobin concentrations may also have attenuation coefficients similar to cardiac muscle.<sup>21</sup>

### CARDIAC TUMOR OR TUMORLIKE LESION

#### Intracardiac Thrombus

Thrombus is the most common intracardiac mass; it typically occurs along the posterolateral wall of the left atrial cavity or within the left atrial appendage. A predisposing condition, such as atrial fibrillation, is usually present and promotes the formation of the thrombus at these locations. Thrombus is also frequently observed in the apex of the dilated LV chamber in patients with chronic ischemic heart disease (Fig. 15). The detection of thrombi in the left cardiac chambers is important because these patients are exposed to the possibility of systemic embolization. CT may be helpful in differentiating a thrombus from other tissues on the basis of density and contrast enhancement. Right-side intracardiac thrombus is usually associated with deep vein thrombosis and pulmonary thromboembolism; it is also related with Behcet's disease or caused by a neoplasm, such as hepatocellular carcinoma or renal cell carcinoma, which invades the vena cava and is relatively well-enhanced (Figs. 16, 17).<sup>22</sup>

#### Myxoma

Cardiac myxoma is a gelatinous tumor that mimics primitive mesenchyma and is histologically distinct from

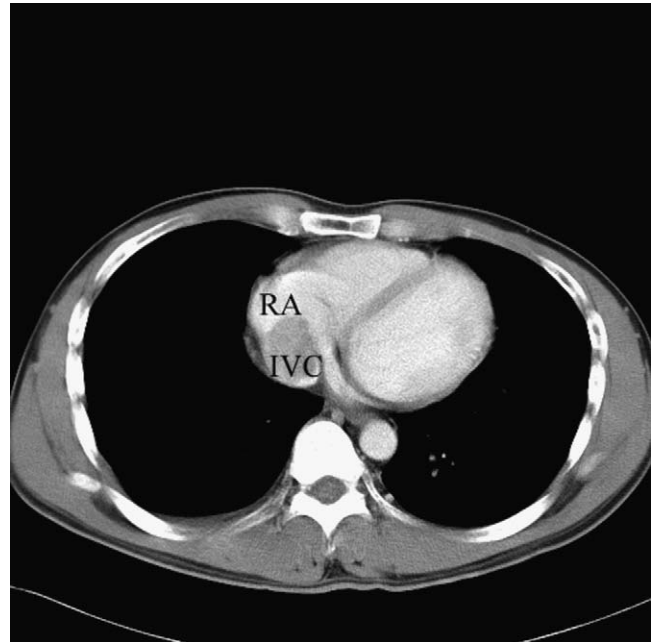


**FIGURE 16.** Tumor thrombus in a 36-year-old man with hepatocellular carcinoma. A large thrombus is noted at the junction of the inferior vena cava (IVC) and the right atrium (RA) in this patient who had a history of hepatocellular carcinoma. Hematogenous metastasis in the lung but not shown in the images.

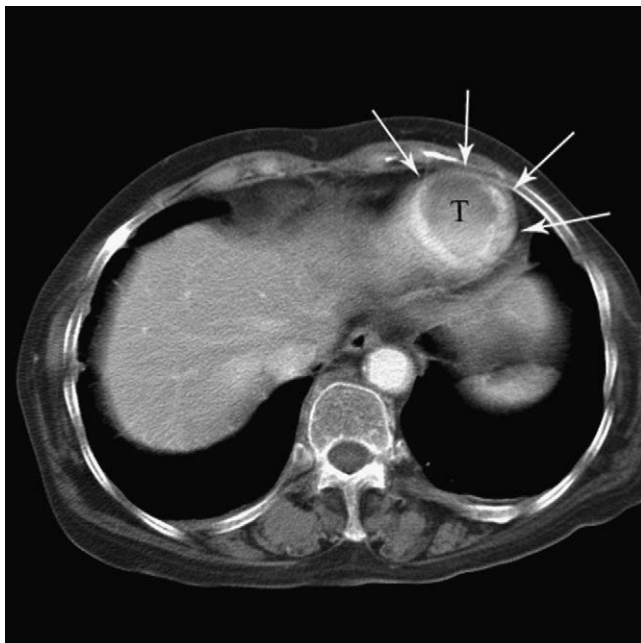


**FIGURE 15.** Thrombus in left a ventricular aneurysm in a 64-year-old woman. An apical aneurysm is noted in the left ventricle. There is large a thrombus (T) in the aneurysmal sac (arrows).

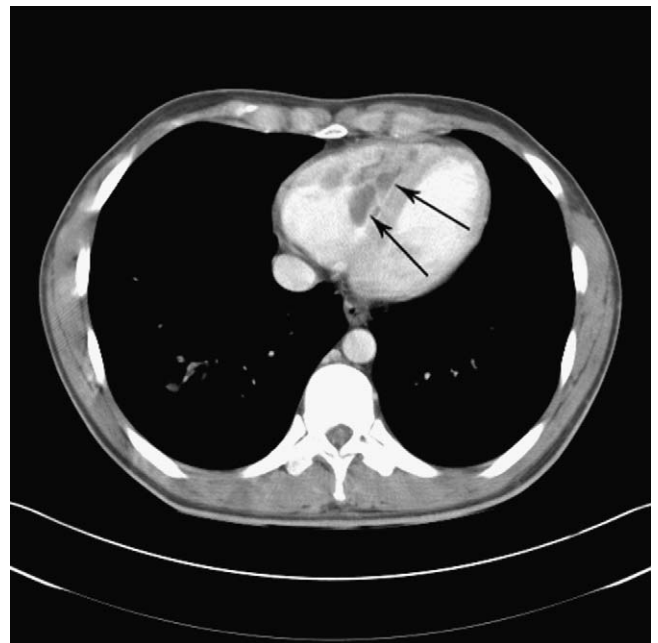


**FIGURE 17.** Intracardiac thrombus in a 25-year-old man with Behcet's disease. A right ventricular thrombus is shown as filling defects (arrows), and there is a thrombus in the right interlobar pulmonary artery (not shown), both of which are characteristic pulmonary manifestations of Behcet's disease.

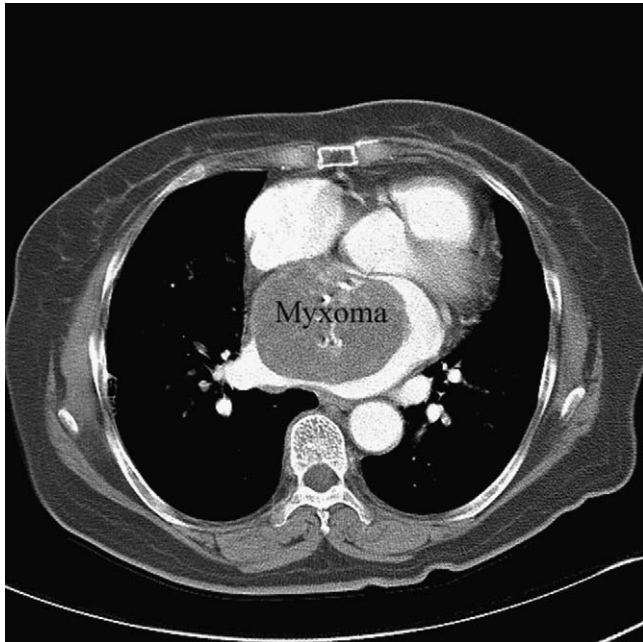


**FIGURE 18.** Left atrial myxoma in a 72-year-old woman. A large myxoma is seen in the right atrium. The heterogeneous mass has multiple calcifications. It is attached to the interatrial septum.

extracardiac soft-tissue myxomas. Myxomas are the most common type of primary cardiac neoplasm. More than 90% of myxomas are solitary, intracavitary, and atrial in location. Myxomas have a predilection for the interatrial

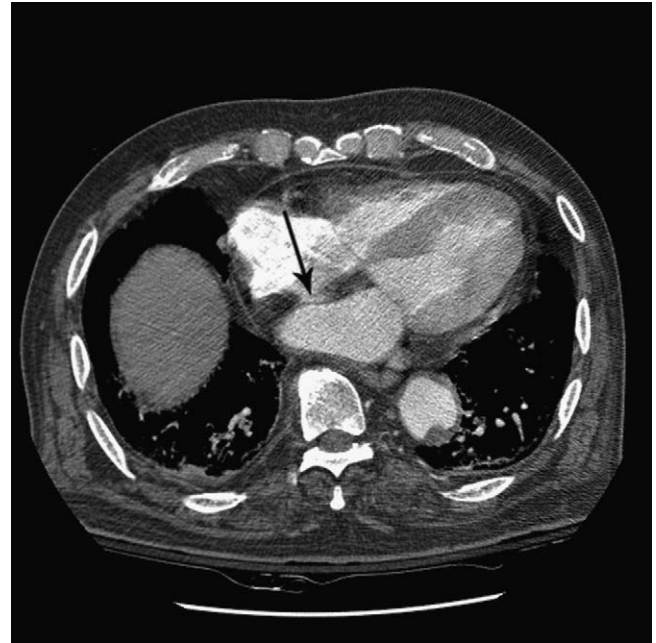


**FIGURE 20.** Lipomatous hypertrophy of the interatrial septum in an 83-year-old man. The interatrial septum is thickened with very low attenuation, which is spared in the fossa ovalis (arrow).

septum. More specifically, they tend to arise from the fossa ovalis. Because of their gelatinous nature, myxomas usually show heterogeneously low attenuation on CT (Fig. 18).<sup>22</sup>

### Lipoma

Primary cardiac lipoma is a benign neoplasm composed of mature adipose tissue; it is histologically similar to extracardiac soft-tissue lipoma. This type of lipoma frequently arises from the epicardial surface, usually from a broad pedicle, and grows into the pericardial space (Fig. 19). They also arise from the endocardium and grow as broad-based, pedunculated masses into any of the cardiac chambers.<sup>23</sup>

### Lipomatous Hypertrophy of the Interatrial Septum

Lipomatous hypertrophy of the interatrial septum is defined as the deposition of fat in the atrial septum at the level of the fossa ovalis. Typically, the fatty infiltration spares the fossa ovalis (Fig. 20). Lipomatous hypertrophy is not a true neoplasm and it is associated with advanced age and obesity and is much more common than cardiac lipoma.<sup>23</sup>

### CONSTRICTIVE PERICARDITIS AND PERICARDIAL CALCIFICATION

Constrictive pericarditis is caused by fibrosis and calcification of the pericardium, processes that inhibit

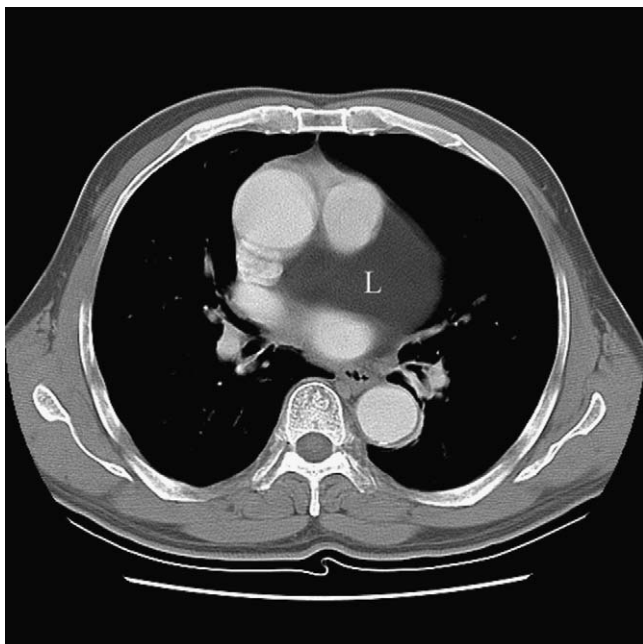


**FIGURE 19.** Cardiac lipoma (L) in a 65-year-old man who underwent CT for lung cancer staging. A large, homogeneous, unenhanced fatty mass is noted in the pericardial space.

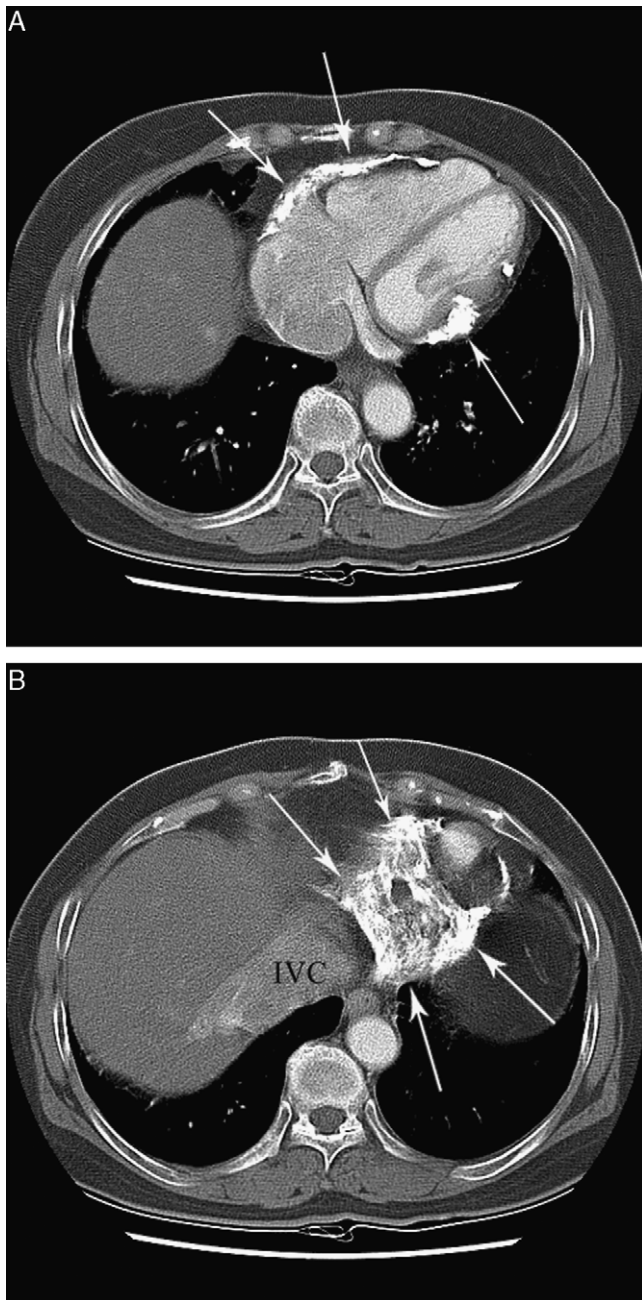


**FIGURE 21.** Constrictive pericarditis in a 65-year-old woman. A, The pericardium is thickened and densely calcified (arrows). The interventricular septum is straightened and the contour of both ventricles is distorted by thick pericardial calcifications. Right atrium is dilated. B, The inferior vena cava (IVC) is dilated and wide calcification band (arrows) is noted along atrioventricular groove.

diastolic filling of the heart. The demonstration of thickened pericardium in the proper clinical setting is basically diagnostic of constriction. Calcification of the pericardium is thought to occur after an inflammatory or traumatic event that leads to fibrocalcific synechiae

between the pericardium and the epicardium. Pericardial calcification may accompany with constrictive physiology, or not. Imaging findings of constrictive pericarditis are dilatation of the inferior vena cava or atria, deformed ventricular contour, tubular-shaped ventricles, angulation of the interventricular septum, ascites, pleural effusion, and pericardial effusion (Fig. 21).<sup>24</sup>

## SUMMARY

Because the clinical manifestations of cardiac and pericardial disease are similar to those of pulmonary diseases and many cardiac and pericardial diseases alter the clinical course or postsurgical outcome in patients with pulmonary disease, the continuing accumulation of knowledge regarding heart disease will allow radiologists to make more accurate and specific CT diagnoses of all thoracic diseases.

## REFERENCES

1. Lipton MJ, Bogaert J, Boxt LM, et al. Imaging of ischemic heart disease. *Eur Radiol.* 2002;23:1061–1080.
2. Arad Y, Spadaro LA, Goodman K, et al. Predictive value of electron beam computed tomography of the coronary arteries. 19-month follow-up of 1173 asymptomatic subjects. *Circulation.* 1996;93:1951–1953.
3. Moore EH, Greenberg RW, Merrick SH, et al. Coronary artery calcifications: significance of incidental detection on CT. *Radiology.* 1989;172:711–716.
4. Shemesh J, Apter S, Itzhak Y, et al. Coronary calcification compared in patients with acute versus in those with chronic coronary events by using dual-sector spiral CT. *Radiology.* 2003; 226:483–488.
5. Brown SL, Gropler RJ, Harris KM. Distinguishing left ventricular aneurysm from pseudoaneurysm: a review of the literature. *Chest.* 1997;111:1403–1409.
6. Robles P, Sonlleve A. Myocardial calcification and subendocardial fatty replacement of the left ventricle following myocardial infarction. *Int J Cardiovasc Imaging.* [Epub ahead of print 2006].
7. Visser CA, Kan G, Meltzer RS, et al. Incidence, timing and prognostic value of left ventricular aneurysm formation after myocardial infarction: a prospective, serial echocardiographic study of 158 patients. *Am J Cardiol.* 1986;57:729–732.
8. Boxt LM, Lipton MJ, Kwong RY, et al. Computed tomography for assessment of cardiac chambers, valves, myocardium and pericardium. *Cardiol Clin.* 2003;21:561–585.
9. Keeley EC, Hillis LD. Left ventricular mural thrombus after acute myocardial infarction. *Clin Cardiol.* 1996;19:83–86.
10. Adler Y, Fink N, Spector D, et al. Mitral annulus calcification—a window to diffuse atherosclerosis of the vascular system. *Atherosclerosis.* 2001;155:1–8.
11. Ha JW, Lee DD, Chung N, et al. Porcelain atrium. *Clin Cardiol.* 2001;24:484.
12. Mahnken AH, Mühlenbruch G, Das M, et al. MDCT detection of mitral valve calcification: prevalence and clinical relevance compared with echocardiography. *AJR.* 2007;188:1264–1269.
13. Roberts WC. Valvular, subvalvular, supra-ventricular aortic stenosis: morphologic features. *Cardiovasc Clin.* 1973;5:97–124.
14. Lippert JA, White CS, Mason AC. Calcification of aortic valve detected incidentally on CT scans: prevalence and clinical significance. *AJR.* 1995;164:73–77.
15. Rozenshtein A, Boxt LM. Computed tomography and magnetic resonance imaging of patients with valvular heart disease. *J Thorac Imaging.* 2000;15:252–264.
16. Steiner RM, Reddy GP, Flicker S. Congenital cardiovascular disease in the adult patient. *J Thorac Imaging.* 2002;17:1–17.

17. Brickner ME, Hillis LD, Lange RA. Congenital heart disease in adults, first of two parts. *N Engl J Med.* 2000;342:256–263.
18. Warnes CA, Libberthson R, Danielson GK, et al. Task force 1: the changing profile of congenital heart disease in adult life. *J Am Coll Cardiol.* 2001;37:1170–1175.
19. Walker F, Webb G. Congenital coronary artery anomalies: the adult perspective. *Coron Artery Dis.* 2001;12:599–604.
20. Conces DJ Jr, Ryan T, Tarver RD. Noncompaction of ventricular myocardium: CT appearance. *AJR.* 1991;156:717–718.
21. Foster M, Nolan RL, Lam M. Prediction of anemia on unenhanced computed tomography of the thorax. *Can Assoc Radiol J.* 2003;54:26–30.
22. Tatli S, Lipton MJ. CT for intracardiac thrombi and tumors. *Int J Cardiovasc Imaging.* 2005;21:115–131.
23. Salanitri JC, Pereles FS. Cardiac lipoma and lipomatous hypertrophy of the interatrial septum: cardiac magnetic resonance imaging findings. *J Comput Assist Tomogr.* 2004;28:852–856.
24. Breen JF. Imaging of the pericardium. *J Thorac Imaging.* 2001;16:47–54.